Supporting Information

Partanen et al. 10.1073/pnas.1120421109

SI Materials and Methods

Animals. All experimental animals were of mixed background and were housed with males from 8 wk of age. They underwent zero to two pregnancies (starting from 8–10 wk of age), after which tumor formation was monitored by palpation and the maximum diameter for a single tumor nodule was set to 15 mm. Mice were genotyped using the primers described below.

Antibodies and Reagents. The following primary antibodies were used: Lkb1 (monoclonal; Abcam); K_i-67 (monoclonal; Dako); phospho-Histone-3 (polyclonal; Cell Signaling); active Caspase-3 (polyclonal; Abcam); ZO-1 (polyclonal; Zymed); Par-3 (polyclonal; Upstate); GM-130 and E-cadherin (monoclonal; BD Transduction Laboratories); Cytokeratin-14 (polyclonal; Covance); desmoplakin (monoclonal; Abcam); EpCAM, Collagen IV, Collagen I, and Collagen III (all polyclonal; Abcam); and Hepsin (polyclonal; Cayman). Antibodies recognizing Laminin-332 and Nidogens 1 and 2 (polyclonal) were kind gifts from Ismo Virtanen (University of Helsinki, Helsinki, Finland). For IF, Alexa-488– and Alexa-546–conjugated secondary antibodies (Invitrogen) were used, and for immunohistochemistry, biotinylated secondary antibodies (Vector Laboratories) were used. The following reagents were used: mouse prolactin and TGF-β1 (R&D Systems), Compound10a (Anix-Chem Limited), GM6001 (Calbiochem), Y-27632 (Calbiochem), and UO1260 and FGF-2 (Sigma).

Cell Culture and Primary Cell Isolation. MMECs were isolated from 8- to 14-wk-old female mice. $Lkb1^{lox/lox}$ and $Lkb1^{+/+}$ MMECs were isolated from littermates. To isolate primary MMECs, number 3, 4, and 5 mammary glands were dissected and finely chopped. The lymph node in number 4 glands was removed. Tissue was incubated with 0.01 mg of Collagenase A (Sigma) per 1 g of tissue in DMEM/F12 media (containing 2.5% FCS, 5 μg/mL insulin, 50 μg/mL gentamicin, and 200 mM glutamine) with gentle shaking (120 rpm in environmental shaker) at 37 °C for 2 h. The resulting cell suspension was then centrifuged at 1,400 rpm/410 × *g* (Heraeus Multifuge 1.0 Rotor #2704) for 10 min and consecutively pulse-centrifuged for six times at 1,400 rpm to get a preparation free of cells other than MMECs. Next, organoids were trypsinized with 0.05% Trypsin-EDTA for 5–10 min to obtain smaller organoid units and drained through a 70-μm cell strainer (Becton Dickinson). Thereafter, cells were counted and plated on low-adhesion plates (Nunc) for adenoviral or lentiviral infections in MMEC growth media [DMEM/F12 media (Gibco) as well as insulin (5 μg/mL), hydrocortisone (1 μg/mL), mouse EGF (10 ng/mL), glutamine (200 mM), gentamicin (50 μg/mL), and penicillin/streptomycin (all from Sigma)] supplemented with 10% (vol/vol) FCS.

Calcium-Switch Assay. Isolated WT MMECs were plated on glass coverslips in normal MMEC growth media and allowed to incubate overnight. On the next day, 4 mM EGTA was added to the medium to chelate calcium for 30 min. After that, EGTA-containing media were removed and replaced with normal MMEC growth media and cells were incubated for 2 h.

Adenoviral Infections. Isolated MMECs were infected on low-adhesion plates with AdCre [or control AdGFP (1)] virus using an MOI of 25 in DMEM/F12 growth media for 18 h. On the next day after the AdCre infection, the mammospheres were washed two to three times with DMEM/F12 growth media. Seventy-two hours after the infection, LKB1 down-regulation was analyzed by Western blotting and the cells were placed in 3D culture.

3D Organotypic Culture. BM from Engelbreth–Holm–Swarm mouse sarcoma (Matrigel; Becton Dickinson) was prepared according to the manufacturer's instructions. MMEC-formed mammospheres were trypsinized with 0.05% Trypsin-EDTA for 5–10 min, centrifuged, suspended with liquid Matrigel, and plated onto eight-chamber slides at ∼1,500 cells per well to form in-Matrigel culture, except for SEM, where cells were seeded on top of Matrigel-coated, eight-chamber slides to form on-Matrigel culture. 3D cultures were grown in DMEM/F12 growth media lacking FCS. For all 3D assays, $Lkb1^{lox/lox}$ and $Lkb1^{+/+}$ MMECs were isolated and pooled from two individual animals in each experiment. IF staining and image acquisition were performed as described earlier (2).

3D IF. The MMEC structures formed in Matrigel were immunostained as described previously (2, 3), with minor modifications. The organotypic cultures were fixed with 2% (wt/vol) paraformaldehyde for 20 min at room temperature (RT) and thereafter washed with PBS. Epithelial structures were permeabilized with 0.25% Triton X-100 in PBS for 10 min at 4 °C and then washed with PBS. The structures were blocked in IF buffer [7.7 mM NaN_3, 0.1% BSA, 0.2% Triton X-100 (Sigma), and 0.05% Tween 20 in PBS] supplemented with 10% (vol/vol) normal goat serum (Gibco) for 1–1.5 h. The primary antibody was incubated in the blocking solution overnight at 4 °C. Following incubation, structures were washed three times with IF buffer (20 min each wash) and then incubated with appropriate Alexa Fluor secondary antibody diluted in IF buffer with 10% goat serum. After 40–50 min of incubation at RT, the structures were washed with IF buffer as before and the nuclei were counterstained with Hoechst 33258 (Sigma). Slides containing immunostained acinar structures were mounted with Immu-Mount reagent (Thermo Scientific). Images of the structures were acquired using a Zeiss LSM Meta 510 confocal microscope equipped with argon (488), helium-neon (543 and 633), and diode (405) lasers. The objectives used were a Plan-Neofluar 40× differential interference contrast (DIC) objective (N.A. = 1.3, oil) and a Plan-Neofluar 63× DIC objective (N.A. = 1.25, oil). Images were arranged using Adobe Photoshop CS5.

Quantification of 3D Structures. Filling of luminal space with cells in MMEC acini was quantified from confocal images. The lumen was defined as cleared, partially cleared, or filled. Apical localization of GM130 and ZO-1 was quantified from confocal images as described in Tables S1–S3. The presence of Collagen IV staining surrounding the 3D acini was quantified either from confocal images or by counting the acini directly under the microscope (Axioplan I upright microscope; Zeiss). Collagen IV staining surrounding the ducts was defined as described in Fig. S2*B*. All quantifications were done from at least three independent experiments counting >10 acini in each experiment. The mean and SD values were also tested with the Student *t* test for statistical significance.

W-Myc Activation in Vivo. MMECs were isolated from virgin W-Myc mice as described above and plated in Matrigel the following day in MMEC growth media lacking FCS. To activate WAP promoter in vitro (4, 5), the 3D structures were treated with a lactogenic hormone mixture (3 μg/mL prolactin, 1 μg/mL hydrocortisone, and 5 μg/mL insulin) as described previously (6) starting from day 1 in 3D culture.

Histopathology, Immunohistochemistry, and TUNEL. Paraffin-embedded tissues (5-μm-thick sections) were deparaffinized and incubated in antigen retrieval solution (Dako) overnight at 70 °C, followed by 1 h of antibody incubation (all other antibodies except Hepsin,

where no antigen retrieval was performed and primary antibody was incubated overnight at 4 °C), standard avidin–biotin complex detection with 3,3-diaminobenzidine (Vector Laboratories), and counterstaining with hematoxylin (Thermo Scientific). TUNEL staining was performed with an ApopTag in situ detection kit (Chemicon/Millipore) according to the manufacturer's instructions. Imaging was performed with a Leica DMB microscope and an Olympus DP50 color camera. Images were processed with Adobe Photoshop.

Quantification of Hepsin Immunostaining in Human Breast Cancer Samples. Hepsin-immunostained samples were visually analyzed for the percentage of tumor area with Hepsin immunostaining and the intensity of immunostaining within these areas. The Hepsin-immunostained percentage was given a score of 0–3 according to the estimated area (0, <15%; 1, 15–40%; 2, 40–70%; 3, >70%). Similarly, the intensity of Hepsin immunostaining was given a score of 0–3 (0, negative; 1, moderate; 2, moderate; 3, strong). The sum of both scores was calculated, and tumors were assigned into groups according to this sum. The analysis was carried out in a blinded fashion independently by two persons.

Whole-Mount Staining of Mammary Gland. Number 4 inguinal mammary glands were fixed in 4% paraformaldehyde overnight and stained for several hours in carmine-alum staining solution (carmine and aluminum potassium sulfate; Sigma). After the desired color had developed, glands were mounted on glass coverslips and imaged.

Tissue IF. Optimal cutting temperature compound (10-μm-thick section; Sakura)-embedded, snap-frozen tissues were fixed in acetone at −20 °C for 10 min and washed twice with PBS for 5 min each wash. Next, slides were permeabilized with 0.25% Triton-X in PBS and incubated in blocking solution [10% (vol/vol) normal goat serum in IF buffer, described above] for 30 min. Primary antibody was incubated in blocking solution for the first 1 h at RT, followed by overnight incubation at 4 °C. Thereafter, slides were washed three times with IF buffer (5 min each time) and incubated with secondary antibody in blocking solution for 1 h at RT. After addition of secondary antibody, slides were again washed three times (5 min each time) and incubated with Hoechst 33258 to counterstain nuclei. Slides were mounted with Immu-Mount reagent and imaged as described for 3D IF staining.

Quantification of Immunohistochemistry and ZO-1 Staining. Eosinophilic areas surrounding mammary ducts were quantitated from images of H&E-stained sections with a magnification of 20×. The diameter of the eosinophilic area was measured from the thickest point using the ImageJ program (National Institutes of Health). A total of 5–20 ducts were quantitated per animal, and 10 animals per genotype were quantitated. For quantification of Collagen IV immunostaining images with magnifications of 20× and 40× were taken from Collagen IV-immunostained sections from 5 to 20 ducts per animal. Collagen IV staining surrounding the ducts was defined as described in Fig S2*B*. Ten animals per genotype were quantified. Apical ZO-1 in mammary ducts was quantitated from confocal IF images as described for 3D MMEC acini (Tables S1–S3). The mean and SD values represent percentages of nuclei with apical ZO-1 in images of >10 individual animals.

EM. 3D acini grown on eight-chamber slides were processed for TEM essentially as previously described (7). Briefly, acini were fixed with 2% (wt/vol) glutaraldehyde in 0.1 M Na-Cacodylate (NaCac) buffer (pH 7.4) for 1.5–2 h at RT and washed subsequently twice with 0.1 M NaCac buffer for 5 min each wash. Thereafter, samples were osmicated with 1% O_SO_4 in 0.1 M NaCac for 1 h and washed with twice with 0.1 M NaCac for 5 min each wash and three times with dH_2O for 10 min each wash. In this step, the wells of the eight-chamber slides were also removed. Next, samples were treated with 1% uranyl acetate-0.3 M sucrose in dH_2O at 4 °C for 1 h and thereafter washed three times with dH_2O for 5 min each wash. Samples were then dehydrated as follows: twice in 70% ethanol (EtOH) for 3 min each time, twice in 96% EtOH for 3 min each time, three times in absolute EtOH for 5 min each time, and twice with acetone for 5 min each time. Next, Epon was dropped onto samples to cover the structures and incubated at RT for 3 h; subsequently, the samples were baked at 60 °C for at least 14 h. After baking, the glass of the eight-chamber slide was removed and samples were cut into 50- to 60-nm-thick sections for imaging. For SEM, samples were treated similarly until dehydration, which was done as follows: one wash for 10 min each from 30%, 50%, 70%, and 96% EtOH and two washes with absolute EtOH. Thereafter, samples were treated in hexamethylsilazane overnight. At least 40 acini per genotype were imaged by SEM in each experiment. By TEM, at least 30 TJs from different acini were quantitated in each experiment.

Genotyping and PCR Analysis of Cre-Mediated Recombination and Primers. The Wap-Cre and Wap-Myc mice were genotyped using the following primers:

Wap-Cre fwd: 5′-TAGAGCTGTGCCAGCCTCTTC-3′
Wap-Cre rev: 5′-CATCACTCGTTGCATCGACC-3′
Wap-Myc fwd: 5′-CACCGCCTACATCCTGTCCATTCAAGC-3′
Wap-Myc rev: 5′-TTAGGACAAGGCTGGTGGGCACTG-3′

The Lkb1 alleles were genotyped using the following primer pairs:

Lkb1_36: 5′-GGGCTTCCACCTGGTGCCAGCCTGT-3′
Lkb1_39: 5′-GAGATGGGTACCAGGAGTTGGGGCT-3′
Lkb1_37: 5′-GATGGAGGACCTCTTGGCCGGCTCA-3′
Lkb1_S5: 5′-TCTAACAATGCGCTCATCGTCATCCTCGGC-3′

Primers 36 and 39 detect the WT allele, primers s5 and 39 detect the conditional lox allele, and primers 36 and 37 detect the deleted null allele (8). The same primers detecting Lkb1 alleles were thus also used as controls when analyzing the Cre-mediated recombination of conditional Lkb1 allele from the mammary gland. The PCR run protocol used for both genotyping the mice and detecting the null allele was as follows: (*i*) 94 °C for 3 min, (*ii*) 94 °C for 30 s, (*iii*) 60 °C for 1 min, (*iv*) 72 °C for 1 min, (*v*) 72 °C for 2 min, and (*vi*) 4 °C; steps *ii*–*iv* were repeated 40 times.

qPCR and Primers. RNA was isolated from MMECs using an RNeasy isolation kit (Qiagen) and from tissues using an AllPrep DNA/RNA kit (Qiagen) according to the manufacturer's instructions. For tissues, homogenization was done using ceramic beads (CK14; Bertin Technologies) and Precellys homogenizer (Bertin Technologies). cDNA synthesis was performed using a DyNAmo cDNA synthesis kit (Finnzymes), and the qPCR reaction was performed using a DyNAmo HS SYBR Green qPCR kit (Finnzymes) and AbiPrism 7500 Fast Real-Time PCR system (Applied Biosystems). Relative mRNA amounts of Lkb1 and β-casein were assayed by comparing PCR cycles with GAPDH using the ΔΔCT method (9) and normalizing the samples to control genotype.

The following run protocol was used with qRT-PCR: (*i*) 50 °C for 10 min, (*ii*) 95 °C for 10 min, (*iii*) 95 °C for 15 s, (*iv*) 60 °C for 45 s, and (*v*) 72 °C for 45 seconds; steps *iii*–*v* were repeated for 40 cycles, and data acquisition was done during step *iv*. The following primers were used. GAPDH primers were from the Harvard primer bank (primer pair ID 6679937a1, http://pga.mgh.harvard.edu/cgi-bin/primerbank): *GAPDH fwd*: 5′-AGGTCGGTGTGAACGGATTTG-3′, *GAPDH rev*: 5′-TGTAGACCATGTAGTTGAGGTCA-3′. Lkb1 quantitative RT-PCR primers have been described before (10).

Lentivirus Production, Vectors, and Constructs. Concentrated lentiviral particles were produced at the Biomedicum Virus Core in a biosafety level 2 laboratory. shRNA constructs targeting Lkb1, Hepsin, and the nontargeting control (shControl, ID no. SHC002) in pLKO.1 lentiviral vector were obtained from the Broad Institute The RNAi Consortium (TRC) library. Sense sequences for the shLkb1 and shHepsin constructs were as follows:

shLkb1-1 (clone ID no.: TRCN0000024146): 5′-CCCAAGGCTGTTTGTGTGAAT-3′
shLkb1-2 (clone ID no.: TRCN0000024145): 5′-GCAGAAGATGTATATGGTGAT-3′
shHepsin (clone ID no.: TRCN00000304737): 5′-CGACTTCTACGGGAATCAGAT-3′

The down-regulation efficiency of the shLkb1 constructs was first verified by viral infection to National Institutes of Health 3T3 cells and Western blotting, after which DNA oligos (from Sigma) containing target sequences for Lkb1 were ordered and cloned into pLL3.7 vector as described previously (11). Hepsin ORF clone without stop codon was obtained in pENTR221-vector (Open Biosystems, Thermo Fisher Scientific, originally from Human ORFeome Collaboration Clones, clone ID no. 100009774). The ORF was then Gateway-cloned with Gateway LR Clonase Plus Enzyme Mix (catalog no. 12538-013; Invitrogen) according to the manufacturer's instructions into a destination vector pLenti6/V5-DEST (Invitrogen).

Lentiviral Infections and Validation of Down-Regulation. Isolated MMECs were infected with concentrated lentiviruses using an MOI of 5 in DMEM/F12 growth media for 18 h. After the lentiviral infections, mammospheres were washed once with PBS and either placed in 3D culture or suspended into PBS containing 10% (vol/vol) FCS for fat pad transplantation. The mice transplanted with transduced MMECs were killed 15 wk after the fat pad transplantation, and MMECs were isolated from four to five glands pooled from different animals as described above. Resulting mammary organoids were either processed as protein lysates or RNA lysates, and the down-regulation of LKB1 was measured by either Western blotting or qPCR as described herein.

Fat Pad Transplantations. Fat pad transplantations were performed essentially as described earlier (12, 13). Three-week-old inbred female FVB mice were anesthetized using isoflurane, and the anterior part of the number 4 mammary gland containing rudimentary ductal epithelium and lymph node was surgically removed. The remaining fat pad was injected with MMECs infected with either shControl or shLkb1 (shLkb1-1 or shLkb1-2) at a rate of 10^5 cells per gland in a 10-μL volume into contralateral glands. Mice were killed as virgins 15 wk after transplantation. The shControl-transduced cells gave rise to outgrowths in 95% of the transduced glands, and the figures were 83% for shLkb1-1 shRNA and 88% for shLkb1-2 shRNA.

Western Blot Analysis and Subcellular Fractionation. MMECs were lysed in ELB lysis buffer [150 mM NaCl, 50 mM Hepes (pH 7.4), 5 mM EDTA, 1% Nonidet P-40] supplemented with EDTA-free protease inhibitor mixture (Roche). For detection of Hepsin, MMECs were lysed in PBS containing 1% Triton-X by letting the lysates stand 15 min on ice and subsequently centrifuging at 13,000 × *g* for 15 min. Mouse mammary glands and tumors and human breast cancer samples were lysed in mammary gland (MG)-lysis buffer (14) supplemented with EDTA-free protease inhibitor mixture. Briefly, a piece of snap-frozen tissue (~2 mm × 2 mm) was placed in a tube containing MG-lysis buffer and ceramic beads (CK14) and homogenized using Precellys homogenizer; subsequently, it was allowed to stand on ice for 30 min and centrifuged at 13,000 × *g* for 15 min. Subcellular fractionation was performed with a Pierce subcellular fractionation kit (Thermo Scientific) according to the manufacturer's instructions. The protein concentration of cell and tissue lysates was determined using a Bio-Rad protein assay. Samples (10 μg) were denatured with 5× Laemmli sample buffer and separated in a 10% (wt/vol) SDS/PAGE gel, and protein bands were blotted into nitrocellulose membrane (Perkin–Elmer).

1. Helenius K, Yang Y, Alasaari J, Mäkelä TP (2009) Mat1 inhibits peroxisome proliferator-activated receptor gamma-mediated adipocyte differentiation. *Mol Cell Biol* 29:315–323.
2. Partanen JI, Nieminen AI, Mäkelä TP, Klefstrom J (2007) Suppression of oncogenic properties of c-Myc by LKB1-controlled epithelial organization. *Proc Natl Acad Sci USA* 104:14694–14699.
3. Debnath J, Muthuswamy SK, Brugge JS (2003) Morphogenesis and oncogenesis of MCF-10A mammary epithelial acini grown in three-dimensional basement membrane cultures. *Methods* 30:256–268.
4. Chen LH, Bissell MJ (1989) A novel regulatory mechanism for whey acidic protein gene expression. *Cell Regul* 1:45–54.
5. Roskelley CD, Srebrow A, Bissell MJ (1995) A hierarchy of ECM-mediated signalling regulates tissue-specific gene expression. *Curr Opin Cell Biol* 7:736–747.
6. Akhtar N, et al. (2009) Molecular dissection of integrin signalling proteins in the control of mammary epithelial development and differentiation. *Development* 136:1019–1027.
7. Seemann J, Jokitalo EJ, Warren G (2000) The role of the tethering proteins p115 and GM130 in transport through the Golgi apparatus in vivo. *Mol Biol Cell* 11:635–645.
8. Bardeesy N, et al. (2002) Loss of the Lkb1 tumour suppressor provokes intestinal polyposis but resistance to transformation. *Nature* 419:162–167.
9. Livak KJ, Schmittgen TD (2001) Analysis of relative gene expression data using real-time quantitative PCR and the 2(-Delta Delta C(T)) Method. *Methods* 25:402–408.
10. Shorning BY, et al. (2009) Lkb1 deficiency alters goblet and paneth cell differentiation in the small intestine. *PLoS ONE* 4:e4264.
11. Nieminen AI, Partanen JI, Hau A, Klefstrom J (2007) c-Myc primed mitochondria determine cellular sensitivity to TRAIL-induced apoptosis. *EMBO J* 26:1055–1067.
12. Welm BE, Dijkgraaf GJ, Bledau AS, Welm AL, Werb Z (2008) Lentiviral transduction of mammary stem cells for analysis of gene function during development and cancer. *Cell Stem Cell* 2:90–102.
13. Deome KB, Faulkin LJ, Jr., Bern HA, Blair PB (1959) Development of mammary tumors from hyperplastic alveolar nodules transplanted into gland-free mammary fat pads of female C3H mice. *Cancer Res* 19:515–520.
14. Zhu Z, Jiang W, Thompson HJ (2003) Mechanisms by which energy restriction inhibits rat mammary carcinogenesis: In vivo effects of corticosterone on cell cycle machinery in mammary carcinomas. *Carcinogenesis* 24:1225–1231.

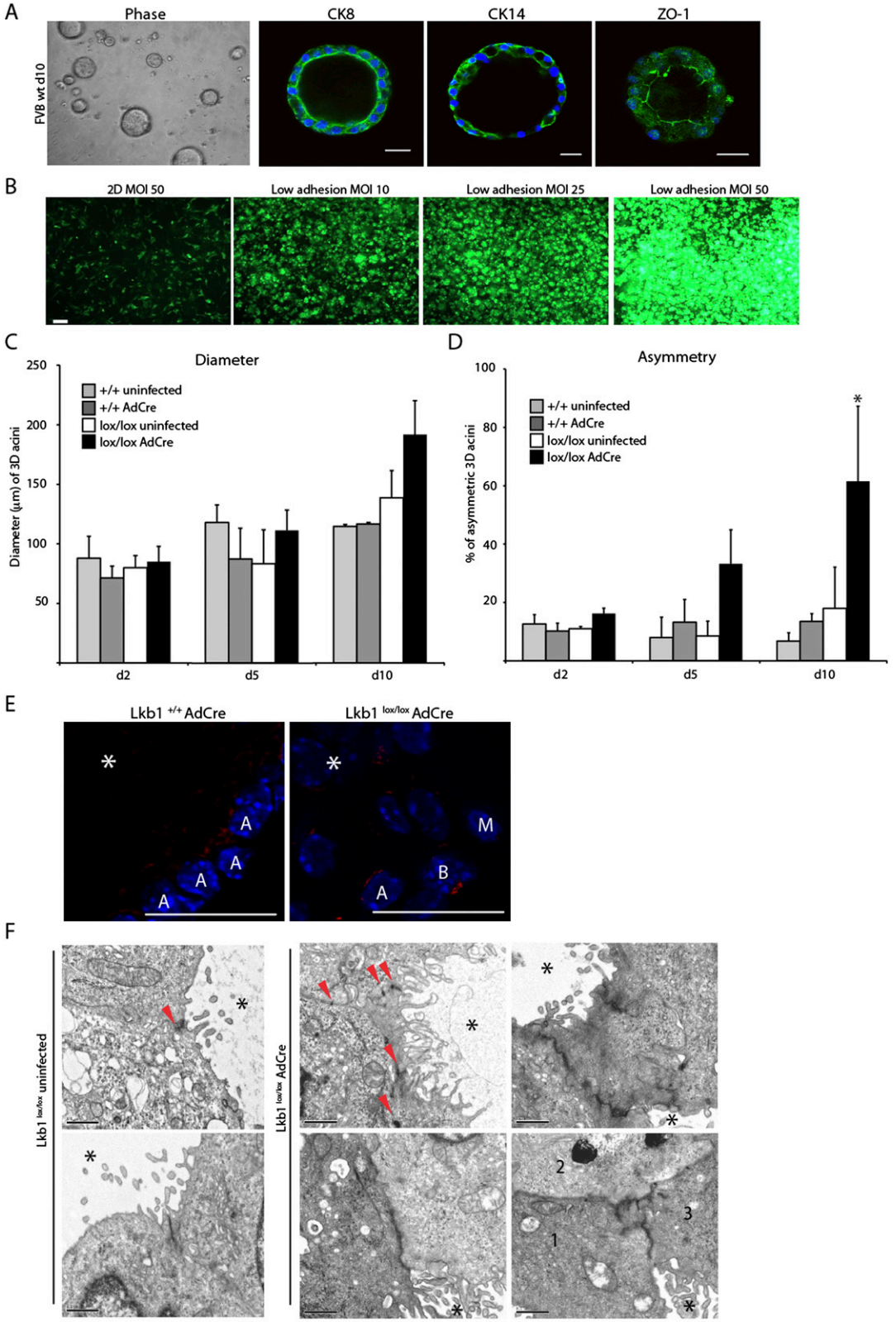

Fig. S1. Conditional deletion of *Lkb1* with AdCre disrupts epithelial architecture and organization of cell junctions. (*A*) MMECs cultured on reconstituted BM (Matrigel) form acinar structures containing cells positive for luminal (CK-8) and myoepithelial (CK-14) markers. These 3D acini contain a hollow lumen and are polarized as indicated by apical ZO-1 staining. (Scale bars: 100 μm in phase-contrast image, 20 μm in IF images.) (*B*) High adenoviral transduction efficiency of MMECs cultured on low-adhesion plates. IF images of MMECs infected with AdGFP virus on a 2D culture plate (leftmost image) or on a low-adhesion plate using different MOIs. (Scale bar: 50 μm.) (*C* and *D*) Quantification of morphological parameters indicates that AdCre-infected Lkb1$^{lox/lox}$ acini were large (diameter of 191.7 ± 28.5 μm vs. 116.7 ± 1.3 μm in Lkb1$^{+/+}$ littermate control acini) and asymmetrical compared with control acini. In 3D assays, mean and SD

Legend continued on following page

values were calculated from at least three independent experiments. (*E*) Examples of images used in analysis of apical polarity. Confocal images demonstrate an apical pattern of GM130 in a control acinus (*Left*) and a nonpolarized pattern in an Lkb1-deficient acinus (*Right*). A, apically localized GM130; B, basally localized GM130; M, missing GM130 staining. An asterisk marks the lumen area. Only cells facing the BM were included in the analysis. (Scale bar: 20 μm.) (*F*) Loss of *Lkb1* disrupts organization of cell junctions. TEM images were taken from AdCre-infected Lkb1$^{lox/lox}$ and uninfected acini grown in Matrigel for 5 d. AdCre-infected Lkb1$^{lox/lox}$ acini had abnormally long, laterally oriented TJs (*Lower*), multiplication of desmosomes (*Upper Center*), occasionally two apical sides attributable to the presence of microlumina (*Upper Right*), and multilayering of cells (*Lower Right*). Red arrowheads mark desmosomes, and asterisks mark lumens. (Scale bar: 0.5 μm.)

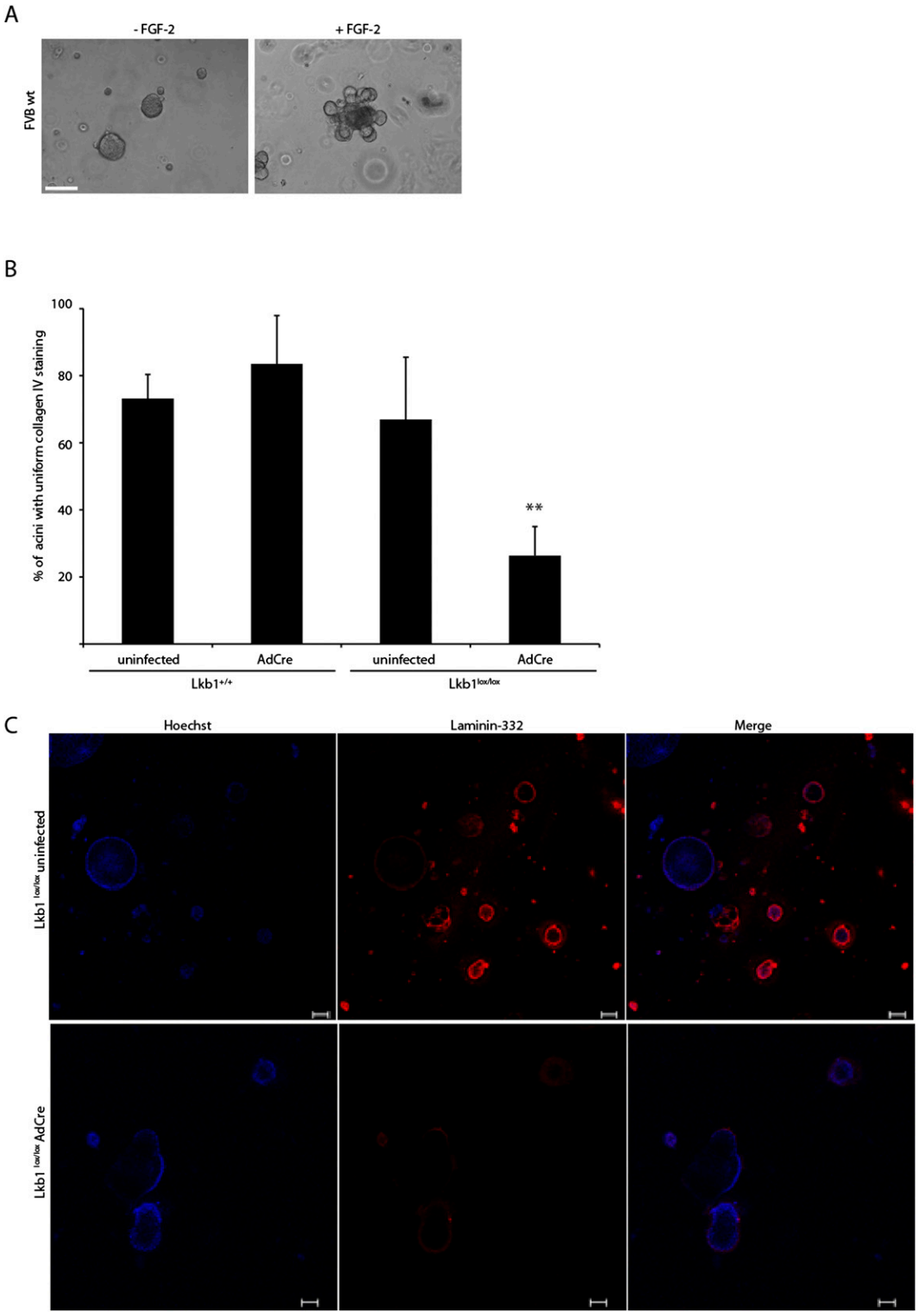

Fig. S2. Branching morphogenesis and quantification of BM in 3D MMEC acini. (*A*) WT 3D MMEC acini grown with or without 2.5 nM FGF-2 for 5 d display branching morphogenesis. (Scale bar: 50 μm.) (*B*) Intactness of BM in 3D acini. For analyses, the acini were classified in four groups depending on the uniformity of Collagen IV staining. The groups were uniform (staining evenly surrounding the acinus), patchy (staining surrounding >50% of the acinus), uneven (staining surrounding <50% of the acinus), or absent (staining missing). Mean and SD values represent three independent experiments. (*C*) Day 10 control and AdCre-infected *Lkb1*$^{lox/lox}$ 3D acini immunostained for Laminin-332 show a discontinuous and reduced staining pattern in LKB1-deficient acini. (Scale bar: 50 μm.)

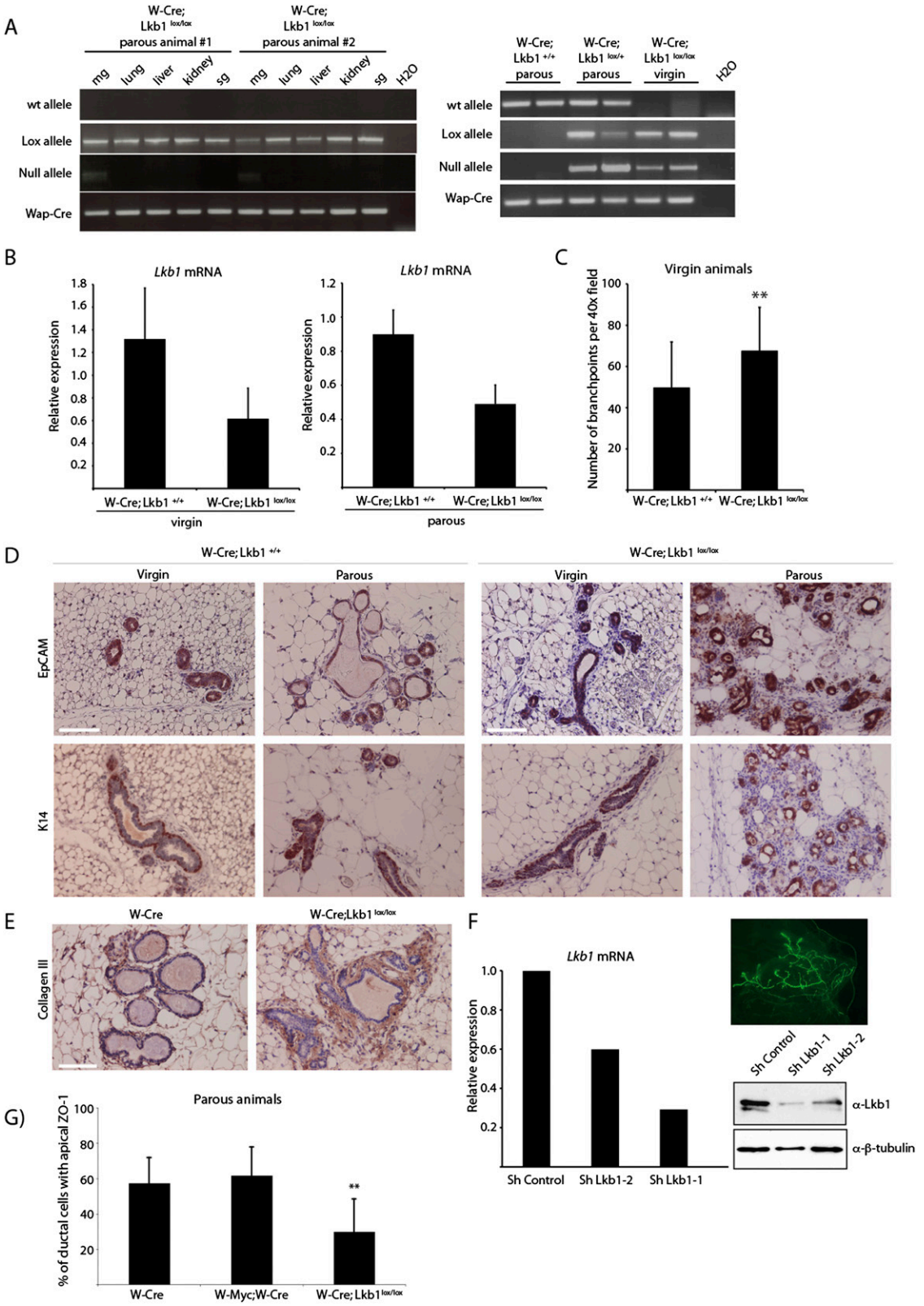

Fig. S3. Validation of *Lkb1* loss in the mouse models and histological analysis. (*A*) Genomic PCR shows recombination of conditional Lox allele into null allele in W-Cre;Lkb1$^{lox/+}$ and W-Cre;Lkb1$^{lox/lox}$ mammary glands. (*Left*) PCR analysis of mammary glands and control organs (lung, liver, kidney, and salivary gland) of two parous W-Cre;Lkb1$^{lox/lox}$ females shows the specific appearance of null Lkb1 allele in mammary glands. WT, conditional (Lox), and W-Cre alleles are used as controls in PCR. (*Right*) PCR analysis of parous W-Cre;Lkb1$^{lox/+}$ and virgin W-Cre;Lkb1$^{lox/lox}$ mammary glands confirms the presence of null Lkb1 allele in hemizygous and nulliparous glands. WT, conditional (Lox), and W-Cre alleles were used as controls for PCR. (*B*) qPCR analysis shows a reduction in Lkb1 mRNA in MMECs isolated from either virgin or parous W-Cre;Lkb1$^{lox/lox}$ mice. (*C*) Increased mammary ductal branching in virgin Lkb1-deficient animals. Carmine-

Legend continued on following page

alum–stained glands were quantitated for branching. Mean and SD values represent the number of branch point in fields with a magnification of 40× counted with the aid of the ImageJ program (3–4 fields counted per animal, >8 animals per group; $P = 0.0099$, Student t test). (*D*) LKB1 deficiency does not induce gross alterations in the function, ultrastructure, or luminal/myoepithelial cell composition of the mammary glands. Epithelial cell adhesion molecule and Cytokeratin 14 immunostaining demonstrates the presence of luminal and myoepithelial cells in ducts of both virgin and parous W-Cre;*Lkb1*$^{lox/lox}$ mammary glands. (Scale bar: 100 μm.) Furthermore, both W-Cre;*Lkb1*$^{lox/+}$ and W-Cre;*Lkb1*$^{lox/lox}$ dams were able to lactate and produce viable litters. (*E*) Overproduction of interstitial Collagen III in virgin W-Cre;*Lkb1*$^{lox/lox}$ mammary glands. (Scale bar: 100 μm.) (*F*) qPCR and Western blot analysis of Lkb1 mRNA and protein in reconstituted mammary ductal tree. The mammary ductal tree was reconstituted from mammary progenitor cells transduced with lentivirus expressing shRNA against Lkb1 (shRNA Lkb1-1 or Lkb1-2) or control shRNA. Knockdown was analyzed in MMECs isolated from glands 15 wk after transplantation. (*Inset*) Image of a ductal tree from genetically engineered progenitor cells. MMECs were transduced with GFP expressing high-titer lentivirus and transplanted into cleared fat pad using a method adapted from Welm et al. (12). The image (0, 71×) shows GFP-positive ductal outgrowths derived from transduced cells 6 wk after transplantation. (*G*) Apical ZO-1 was quantitated as described in *SI Materials and Methods* in frozen sections of parous W-Cre;*Lkb1*$^{lox/lox}$ and control mice (W-Cre and W-Cre;W-Myc; see below). Ten animals per group were quantitated.

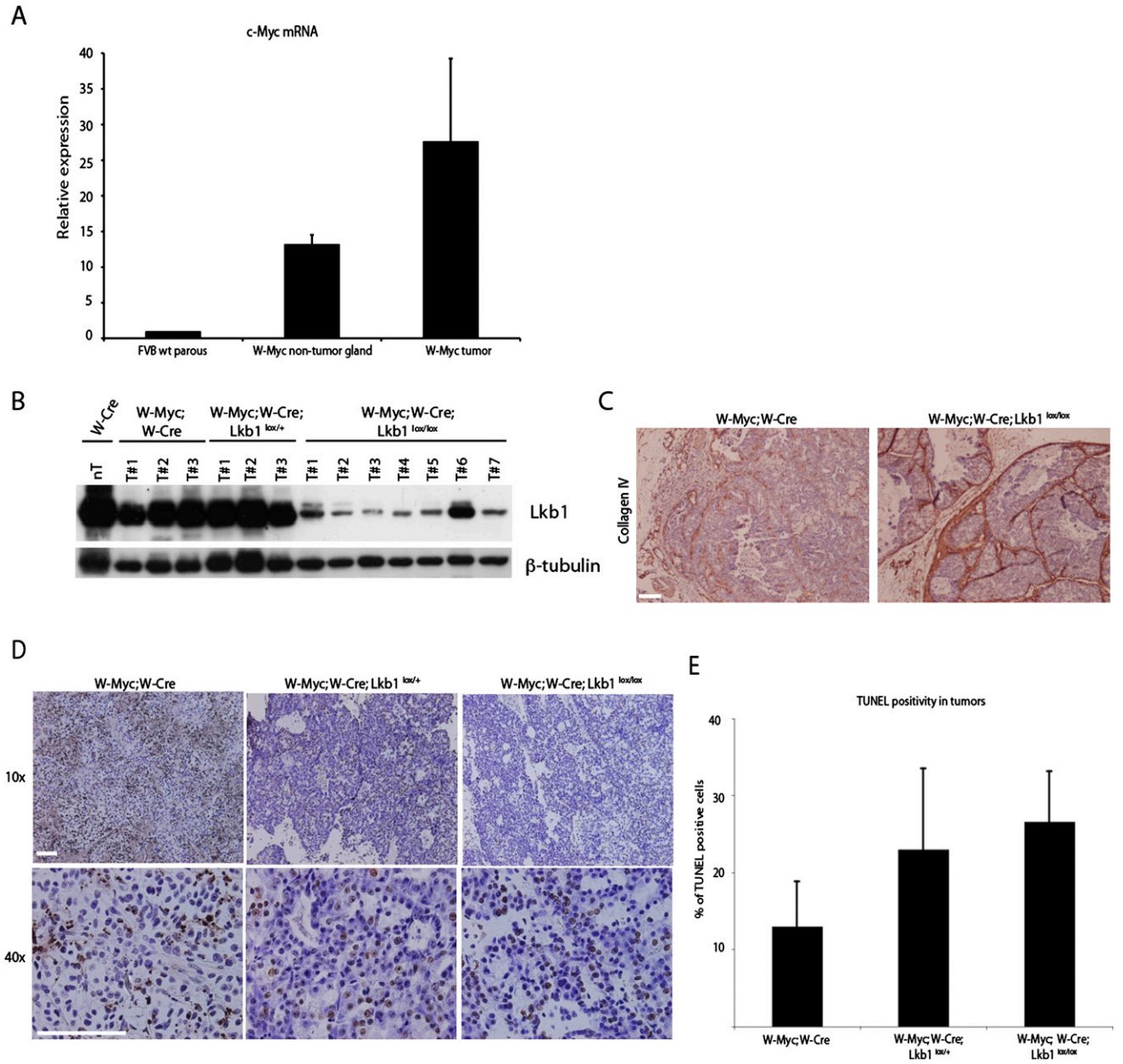

Fig. S4. Validation of Myc overexpression/loss of Lkb1, histological analysis of BM, and quantification of apoptosis in mammary tumors from W-Myc;W-Cre; *Lkb1*$^{lox/lox}$ mice. (*A*) qPCR analysis of Myc mRNA isolated from nontumorous glands or tumors from parous W-Myc mice shows a >10-fold increase in Myc mRNA in nontumorous glands and a >25-fold increase in tumors. (*B*) Western blot analysis of LKB1 protein levels in mammary tumors (T#) from W-Myc;W-Cre, W-Cre; W-Myc;*Lkb1*$^{lox/+}$, and W-Myc;W-Cre;*Lkb1*$^{lox/lox}$ mice. (*C*) (*Left*) Invasive adenocarcinoma from a W-Myc;W-Cre mouse lacking BM as indicated by the absence of Collagen IV immunostaining. (*Right*) In comparison, an MIN tumor from a W-Cre;W-Myc;*Lkb1*$^{lox/lox}$ mouse. These tumors had undisrupted BM in the area where the tumor mass was facing the stroma. Deteriorating BM inside the tumor was commonly observed. (Scale bar: 200 μm.) (*D*) TUNEL staining of W-Myc;W-Cre, W-Myc;W-Cre;*Lkb1*$^{lox/+}$, and W-Myc;W-Cre;*Lkb1*$^{lox/lox}$ tumors shows similar amounts of apoptotic cells in all samples. (Scale bar: 100 μm.) (*E*) Quantification of TUNEL positivity (n = 11 in all groups).

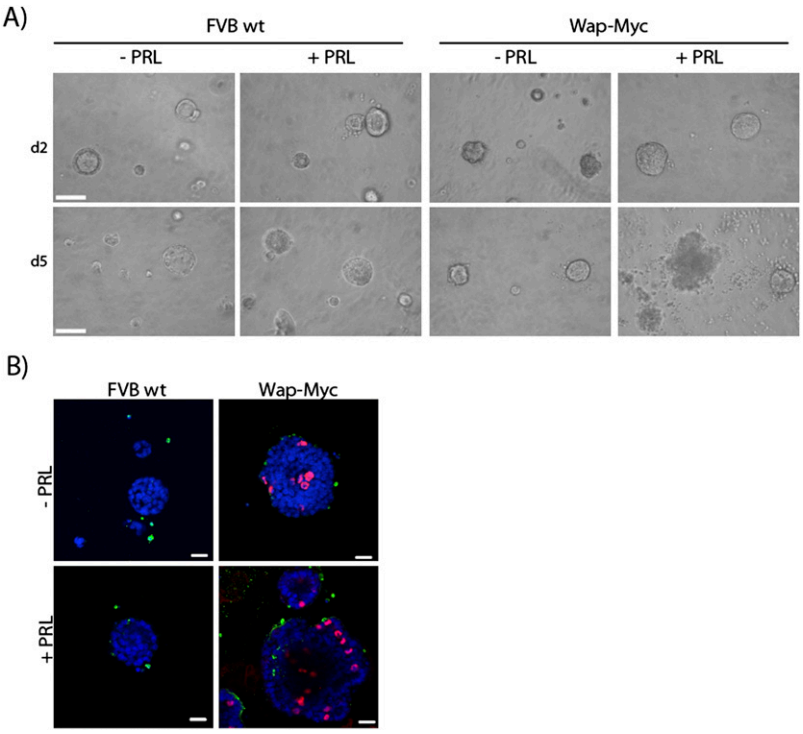

Fig. S5. W-Myc is biologically active in vitro without lactogenic hormone induction. (*A*) Morphology of W-Myc acini is transformed without lactogenic hormone treatment. WT type inbred FVB and W-Myc MMECs were grown in Matrigel for 2 or 5 d in the absence (−PRL) or presence (+PRL) of a lactogenic hormone mixture. The untreated W-Myc acini exhibited filling of luminal space, enhanced proliferation, and apoptosis, all indicative of functional Myc activity. Lactogenic hormone treatment enhanced transformation in W-Myc acini; however, these structures succumbed to apoptosis after day 5 in culture. (Scale bar: 50 μm.) (*B*) Enhanced proliferation and apoptosis in both untreated (−PRL) and treated (+PRL) W-Myc 3D MMEC acini grown in Matrigel for 5 d. The structures were immunostained with antibodies recognizing phospho-Histone-3 and active Caspase-3 to analyze proliferation and apoptosis, respectively. (Scale bar: 20 μm.)

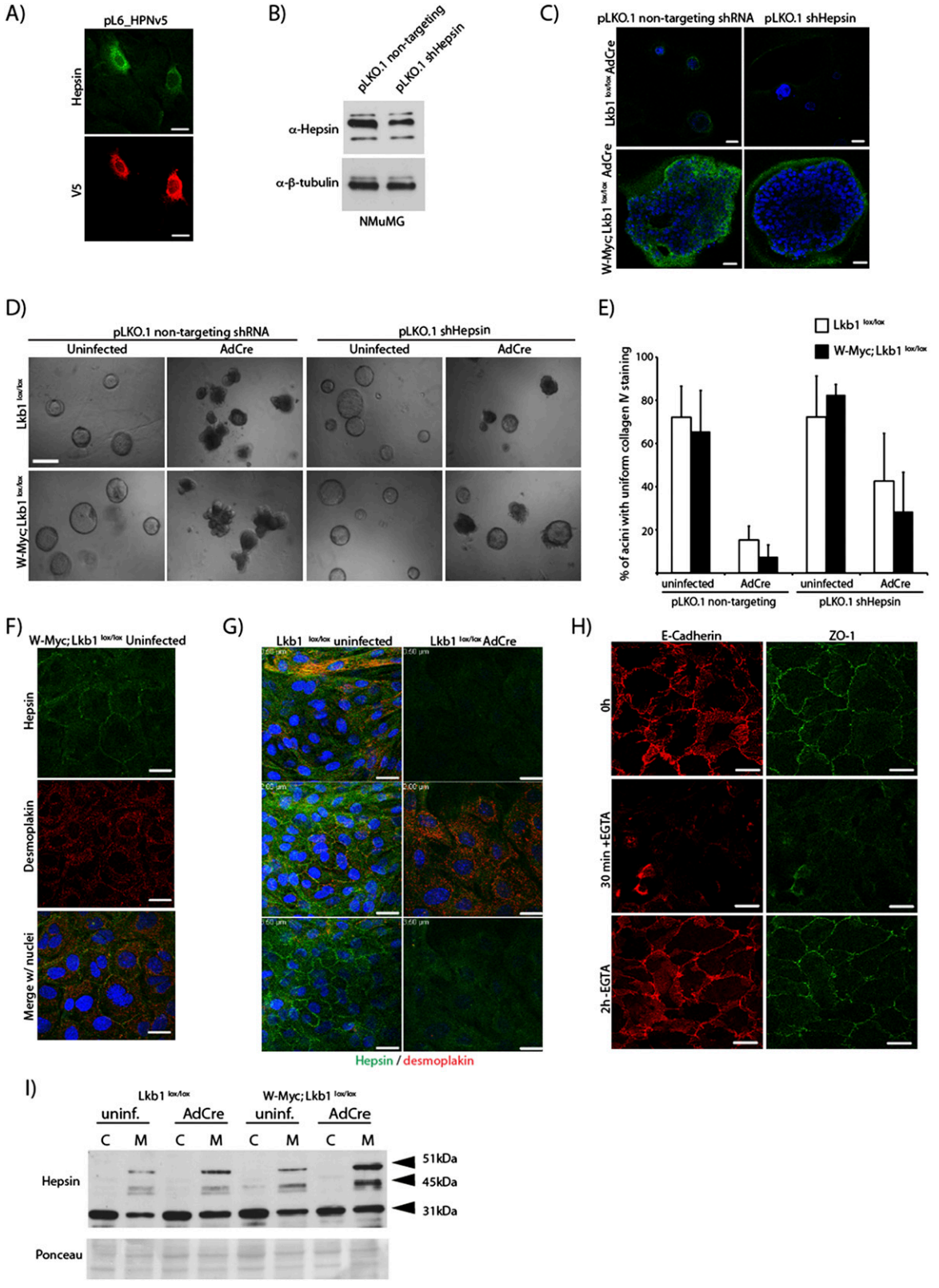

Fig. S6. Genetic manipulation of Hepsin and effects in Lkb1-deficient MMECs. (*A*) WT MMECs transduced with lentiviral pL6_HPNV5 expression construct show a diffuse cytosolic staining pattern. Hepsin overexpression is visualized by antibodies against Hepsin and V5 tag. (*B*) Western blot analysis of shRNA-mediated Hepsin silencing in unselected NMuMG MMEC line after transduction with pLKO.1 shHepsin or control lentivirus. (*C*) IF staining demonstrates silencing of Hepsin in day 10 3D *Lkb1*$^{lox/lox}$ and W-Myc;*Lkb1*$^{lox/lox}$ MMEC acini. MMECs were infected with AdCre and pLKO.1 shHepsin or control lentivirus immediately before 3D culture. (*Lower Right*) Green staining is background from Matrigel. (Scale bar: *Upper*, 50 μm; *Lower*, 20 μm.). (*D*) Silencing of Hepsin partially reverses epithelial phenotypes induced by loss of Lkb1 and Myc + Lkb1 loss double lesions. Phase-contrast images of day 10 *Lkb1*$^{lox/lox}$ and W-Myc;

Legend continued on following page

Lkb1$^{lox/lox}$ MMEC acini infected with AdCre and pLKO.1 shHepsin or control shRNA carrying lentivirus. (Scale bar: 100 μm.) (*E*) Silencing of Hepsin partially reverses BM defect induced by loss of Lkb1 or Myc + Lkb1 loss double lesion in 3D acini. Intactness of BM was quantitated as in Fig S2*B*. Mean and SD are from three independent experiments. (*F*) Additional control to Fig. 7*I*. Uninfected W-Myc;*Lkb1*$^{lox/lox}$ MMECs show a normal pattern of Hepsin and desmoplakin staining at cell-cell borders. (Scale bar: 20 μm.) (*G*) Confocal z-stack showing three focal planes (at 1.5-μm interval) further confirms lack of colocalization of desmoplakin and Hepsin and loss of desmoplakin at cell-cell borders in Lkb1-deficient MMECs. (Scale bar: 20 μm.) (*H*) Dissociation of ZO-1 and E-cadherin from cell-cell borders in a calcium switch assay. (Scale bar: 20 μm.) (*I*) Western blot analysis showing expression of Hepsin proforms and processed form (31 kDa) in cytosolic and membrane fractions from *Lkb1*$^{lox/lox}$ and W-Myc;*Lkb1*$^{lox/lox}$ MMECs. C, cytosolic fraction; M, membrane fraction consisting of plasma and intracellular membranes. Ponceau staining shows equal loading.

Table S1. Quantitative measures of 3D MMEC structures: Degree of luminal filling with cells

Genotype	Acini with lumen filled with cells, %	SD	*P* value
Lkb1$^{+/+}$ uninfected	22.02	19.59	
Lkb1$^{+/+}$ AdCre	25.00	25.00	
Lkb1$^{lox/lox}$ uninfected	16.19	14.66	
Lkb1$^{lox/lox}$ AdCre	64.39	16.36	<0.05

Confocal images were taken from the middle part of the 3D structures. Cells in the lumen area were visualized by Hoechst staining. The lumen area was defined as empty, partially filled with cells, or filled with cells. Mean and SD values were calculated from at least three independent experiments.

Table S2. Quantitative measures of 3D MMEC structures: Apical GM130

Genotype	Acinar rim cells with apical GM130, %	SD	*P* value
Lkb1$^{+/+}$ uninfected	61.40	10.59	
Lkb1$^{+/+}$ AdCre	63.22	17.42	
Lkb1$^{lox/lox}$ uninfected	63.05	2.43	
Lkb1$^{lox/lox}$ AdCre	19.92	2.17	<0.05

Apical localization of GM130 was quantitated from confocal images of acini by counting the number of cells with apical GM130 staining among the cells facing BM (rim). Cells exhibiting lateral or basal GM13 were defined as nonapical, and cells with no GM130 staining were left out from quantification. Mean and SD values were calculated from at least three independent experiments.

Table S3. Quantitative measures of 3D MMEC structures: Apical ZO-1 in 3D acini

Genotype	Acinar rim cells with apical ZO-1, %	SD	*P* value
Lkb1$^{+/+}$ uninfected	73.41	12.40	
Lkb1$^{+/+}$ AdCre	63.39	21.24	
Lkb1$^{lox/lox}$ uninfected	76.52	12.15	
Lkb1$^{lox/lox}$ AdCre	18.69	3.13	<0.005

Apical localization of ZO-1 was quantitated from confocal images of acini as above. Mean and SD values were calculated from at least three independent experiments.

Table S4. Quantitative measures of histology: Eosinophilic thickenings surrounding mammary ducts

Genotype	Mean thickening diameter, μm	SD	*P* value
W-Cre;*Lkb1*$^{+/+}$	5.59	2.19	
W-Cre;*Lkb1*$^{lox/lox}$	13.08	5.28	<0.05

Images from H&E-stained sections were taken with an objective with a magnification of 20× from 5 to 20 ducts per animal. Eosinophilic regions surrounding the ducts were measured from the thickest point using the ImageJ program. Ten animals per genotype were quantified.

Table S5. Quantitative measures of histology: Intactness of Collagen IV surrounding mammary ducts

Genotype	Ducts with uniform Collagen IV staining, %	SD	*P* value
W-Cre;*Lkb1*$^{+/+}$	65.48	15.66	
W-Cre;*Lkb1*$^{lox/lox}$	43.08	14.62	<0.05

Images from Collagen IV-immunostained sections were taken with an objective with a magnification of 20× from 5 to 20 ducts per animal. Collagen IV staining surrounding the ducts was defined as uniform (100%), patchy (>50%), uneven (<50%), or absent as in Fig. S2*B*. Ten animals per genotype were quantitated.

Table S6. Histopathological analysis of tumors from W-Myc;W-Cre, W-Cre;W-Myc;*Lkb1*$^{lox/+}$, and W-Myc;W-Cre;*Lkb1*$^{lox/lox}$ mice

Genotype	Animal no.	Tumor no.	Biological potential	Morphological descriptors	Property, atypia	Topography	Necrosis, %	Lung metastases	Phenotypic markers, K_i-67, %
W-Myc;W-Cre	MC33	L1	Adenocarcinoma	Cribriform	3	n/a	80	No	80 (+++)
W-Myc;W-Cre	MC33	R5	Adenocarcinoma	Cribriform	3	Focal	80	No	70 (+++)
W-Myc;W-Cre	MC34	2	Adenocarcinoma	Solid	3	Focal	Neg (<5)	No	50 (+++)
W-Myc;W-Cre	MC141	4	Adenocarcinoma	Acinar	3	Focal	Neg (<5)	No	55 (+++)
W-Myc;W-Cre	MC117	1	Adenocarcinoma	Papillary	3	Multifocal	10	No	70 (+++)
W-Myc;W-Cre	MC94	1	Adenocarcinoma	Solid	3	Focal	40	No	65 (+++)
W-Myc;W-Cre	MC85	2	Adenocarcinoma	Solid	3	Focal	Neg (<5)	No	70 (+++)
W-Myc;W-Cre	MCL139	3	Adenocarcinoma	Glandular	3	Focal	20	No	60 (+++)
W-Myc;W-Cre	MCL83	1	Adenocarcinoma	Glandular	3	Focal	Neg (<1)	Yes	80 (+++)
W-Myc;W-Cre;lox/+	MCL22	4	Adenocarcinoma	Cribriform	3	n/a	20	No	40 (+++)
W-Myc;W-Cre;lox/+	MCL55	1	Adenocarcinoma	Solid	3	Focal	10	No	70 (+++)
W-Myc;W-Cre;lox/+	MCL117	4	Adenocarcinoma	Glandular	3	Multifocal	15	No	70 (+++)
W-Myc;W-Cre;lox/+	MCL117	2	Adenocarcinoma	Solid	3	Multifocal	10	No	50 (+++)
W-Myc;W-Cre;lox/+	MCL26	4	Adenocarcinoma	Glandular	3	Focal	20	No	40 (+++)
W-Myc;W-Cre;lox/+	MCL55	3	Adenocarcinoma	Glandular	3	Multifocal	Neg (<5)	No	30 (+++)
W-Myc;W-Cre;lox/+	MCL134	3	Adenocarcinoma	Glandular	3	Focal	5	Yes	n/a
W-Myc;W-Cre;lox/+	MCL134	4	Adenocarcinoma	Glandular	3	Focal	10	(Yes)	50 (+++)
W-Myc;W-Cre;lox/+	MCL22	3	Adenocarcinoma	Glandular	3	Focal	15	No	n/a
W-Myc;W-Cre;lox/lox	MCL130	1	MIN	NOS	3	Diffuse	15	No	20 (++)
W-Myc;W-Cre;lox/lox	MCL130	3	MIN	NOS	3	Diffuse	20	No	35 (+++)
W-Myc;W-Cre;lox/lox	MCL130	5	MIN	NOS	3	Diffuse	Neg (5)	No	40 (+++)
W-Myc;W-Cre;lox/lox	MCL130	8	MIN	NOS	3	Diffuse	Neg (2)	No	40 (+++)
W-Myc;W-Cre;lox/lox	MCL133	6	MIN	NOS	3	Diffuse	Neg (<5)	No	35 (+++)
W-Myc;W-Cre;lox/lox	MCL133	7	MIN	NOS	3	Diffuse	20	No	35 (+++)
W-Myc;W-Cre;lox/lox	MCL25b	6	Adenocarcinoma	Cribriform	3	Diffuse	10	No	60 (+++)
W-Myc;W-Cre;lox/lox	MCL63b	3	Adenocarcinoma	NOS	3	Diffuse	10	No	70 (+++)
W-Myc;W-Cre;lox/lox	MCL61b	6	Adenocarcinoma	Glandular	3	Diffuse	10	No	60 (+++)
W-Myc;W-Cre;lox/lox	MCL61b	1	Adenocarcinoma	Glandular	3	Diffuse	10	No	50 (+++)
W-Myc;W-Cre;lox/lox	MCL24b	2	Adenocarcinoma	Glandular	3	Multifocal	10	No	50 (+++)
W-Myc;W-Cre;lox/lox	MCL85a	4	MIN	NOS	3	Diffuse	3	No	40 (+++)
W-Myc;W-Cre;lox/lox	MCL85a	5	MIN	NOS	3	Diffuse	5	No	50 (+++)
W-Myc;W-Cre;lox/lox	MCL18c	2	Adenocarcinoma	NOS	3	Diffuse	5	No	25 (++)
W-Myc;W-Cre;lox/lox	MCL18c	3	Adenocarcinoma	Glandular	3	Diffuse	1	No	60 (+++)
W-Myc;W-Cre;lox/lox	MCL56b	1	MIN	Cribriform	3	Diffuse	2	No	65 (+++)
W-Myc;W-Cre;lox/lox	MCL56b	3	MIN	Cribriform	3	Diffuse	<1	No	80 (+++)
W-Myc;W-Cre;lox/lox	MCL96b	3	Adenocarcinoma	Solid	3	Diffuse	20	No	80 (+++)
W-Myc;W-Cre;lox/lox	MCL43b	4	Adenocarcinoma	Glandular	3	Diffuse	5	No	30 (+++)

++, 20–30 % Ki67 positive cells; +++, >30% Ki67 positive cells.

Tumors were analyzed from H&E-stained sections according to Annapolis meeting recommendations for mammary pathology of genetically engineered mice (1). The parameters included biological potential (adenocarcinoma/MIN), morphological descriptor (glandular structure visible, as in either glandular or acinar cribriform, or not, as in solid type), atypia (scored from 1 to 3 according to nuclear pleiomorphy, nuclear-to-cytoplasm ratio, and high mitotic frequency), and topography (focal, multifocal, or diffuse). Additionally, the amount of necrosis and K_i-67 positivity in the tumors and possible lung metastases in the mice was recorded. n/a, not applicable; Neg., negative; NOS, not otherwise specified.

1. Cardiff RD, et al. (2000) The mammary pathology of genetically engineered mice: The consensus report and recommendations from the Annapolis meeting. *Oncogene* 19:968–988.

Table S7. Histopathology of analyzed human breast cancer samples

Tumor type	Grade	Hepsin, %	H_Intensity	Sum	Lkb1 diminished
Ductal carcinoma	G3	2	1	3	Yes
Ductal carcinoma	G3	2	1	3	
Ductal carcinoma	G2	1	1	2	Yes
Ductal carcinoma	G1	1	1	2	Yes
Ductal carcinoma	G2	1	1	2	
Ductal carcinoma	G2	1	1	2	
Ductal carcinoma	G3	2	1	3	
Lobular carcinoma	G3	1	1	2	
Ductal carcinoma	G1	2	1	3	Yes
Ductal carcinoma	G2	3	2	5	Yes
Ductal carcinoma	G3	1	1	2	Yes
Lobular carcinoma	G2	2	1	3	
Ductal carcinoma	G2	0	0	0	
Ductal carcinoma	G3	2	1	3	
Ductal carcinoma	G3	0	0	0	
Ductal carcinoma	G2	0	0	0	
Ductal carcinoma	G3	0	0	0	
Ductal carcinoma	G2	1	1	2	Yes
Ductal carcinoma	G1	1	1	2	Yes
Ductal carcinoma	G3	1	1	2	
Ductal carcinoma	G3	0	0	0	
Ductal carcinoma	G3	0	0	0	
Ductal carcinoma	G3	3	1	4	
Ductal carcinoma	G3	0	0	0	
Ductal carcinoma	G1	1	1	2	
Ductal and lobular carcinoma	G3	3	1	4	Yes
Ductal and lobular carcinoma	G2	1	1	2	
Ductal and lobular carcinoma	G1	3	2	5	Yes
Ductal carcinoma	G2	1	1	2	
Ductal carcinoma	G3	0	0	0	
Ductal carcinoma	G1	3	1	4	
Ductal carcinoma	G3	3	2	5	
Ductal carcinoma	G2	3	1	4	
Cribriform carcinoma	G1	3	1	4	
Ductal carcinoma	G2	3	3	6	
Ductal carcinoma	G1	2	1	3	
Lobular carcinoma	G1	3	2	5	
Lobular carcinoma	G2	2	1	3	
Ductal carcinoma	G1	2	1	3	
Ductal carcinoma	G3	1	1	2	
Ductal carcinoma	G3	2	1	3	
Ductal carcinoma	G3	1	1	2	
Ductal carcinoma	G2	1	1	2	
Ductal carcinoma	G3	0	0	0	
Ductal carcinoma	G2	0	0	0	
Ductal carcinoma	G3	2	2	4	
Ductal carcinoma	G3	1	1	2	
Ductal carcinoma	G3	3	1	4	
Ductal carcinoma	G3	1	1	2	
Ductal carcinoma	G3	3	3	6	Yes
Ductal carcinoma	G3	2	1	3	
Ductal carcinoma	G3	3	1	4	
Lobular carcinoma	G2	2	1	3	Yes
Ductal carcinoma	G3	3	1	4	Yes
Mucinous carcinoma	G2	3	2	5	Yes
Ductal carcinoma	G3	0	0	0	
Adenosquamous carcinoma	G1	3	1	4	Yes

The area (Hepsin, %) and intensity (H_Intensity) of Hepsin immunostaining were analyzed by a pathologist (P.K.) as described in *SI Materials and Methods*.